Tomatis et al., http://www.jcb.org/cgi/content/full/jcb.201204092/DC1

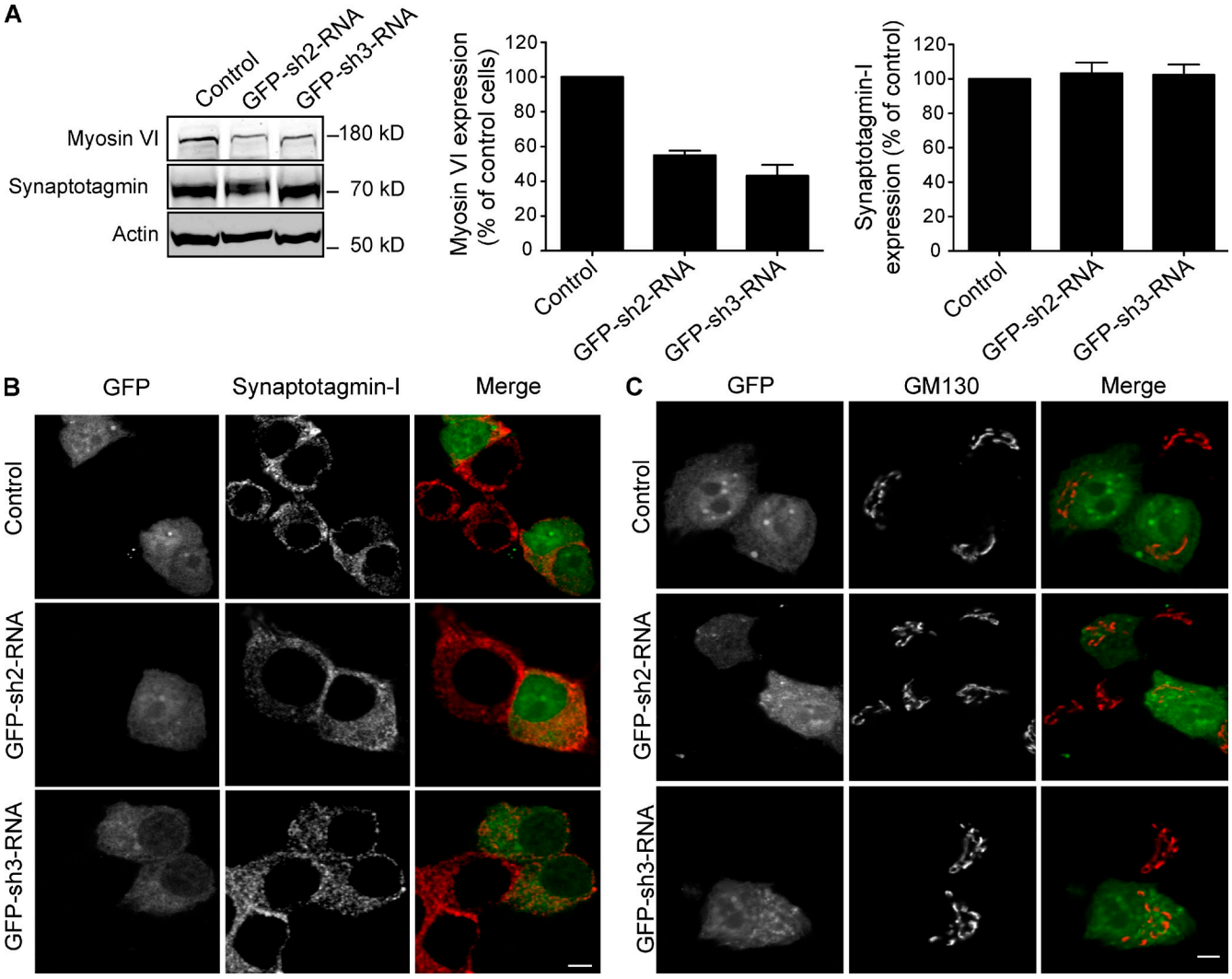

Figure S1. **Myosin VI knockdown does not affect SG biogenesis or Golgi organization.** (A, top) Analysis of Synaptotagmin-I expression levels by Western blotting using an anti–Synaptotagmin-I antibody in cells transfected with GFP–scrambled shRNA (control) or with GFP-shRNA against myosin VI (GFP–sh2-RNA and GFP–sh3-RNA). β-Actin was blotted as a loading control (n = 4). Error bars are means ± SEM. (B and C) Cells transfected with GFP–scrambled shRNA (control) or with GFP-shRNA against myosin VI were fixed and immunostained with anti–Synaptotagmin-I (red; B) or anti-GM130 (C) antibodies and imaged by confocal microscopy. Bars, 5 µm.

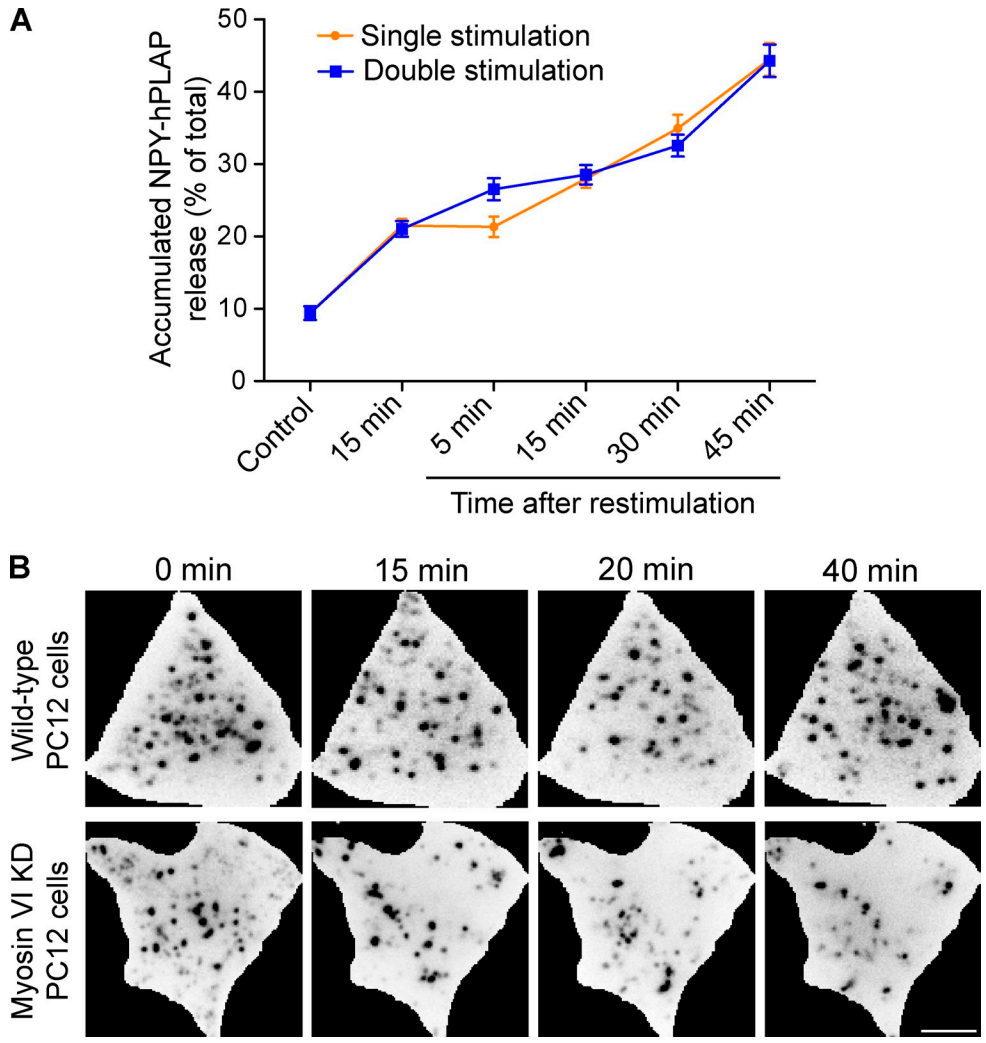

Figure S2. **Myosin VI knockdown affects SG replenishment after stimulation.** (A) Comparison of NPY-hPLAP release in control PC12 cells in response to a long single prolonged stimulation or a double-stimulation protocol. Curves were compared using two-way analysis of variance, revealing no significant difference ($P = 0.6$). Error bars are means ± SEM. (B) Wild-type or myosin VI knockdown (KD) PC12 cells expressing NPY-mCherry were imaged at 1 frame/2 s for 40 min by TIRF microscopy after a single high K^+ stimulation. Images are representative of the SG density at each time point. Bar, 5 µm.

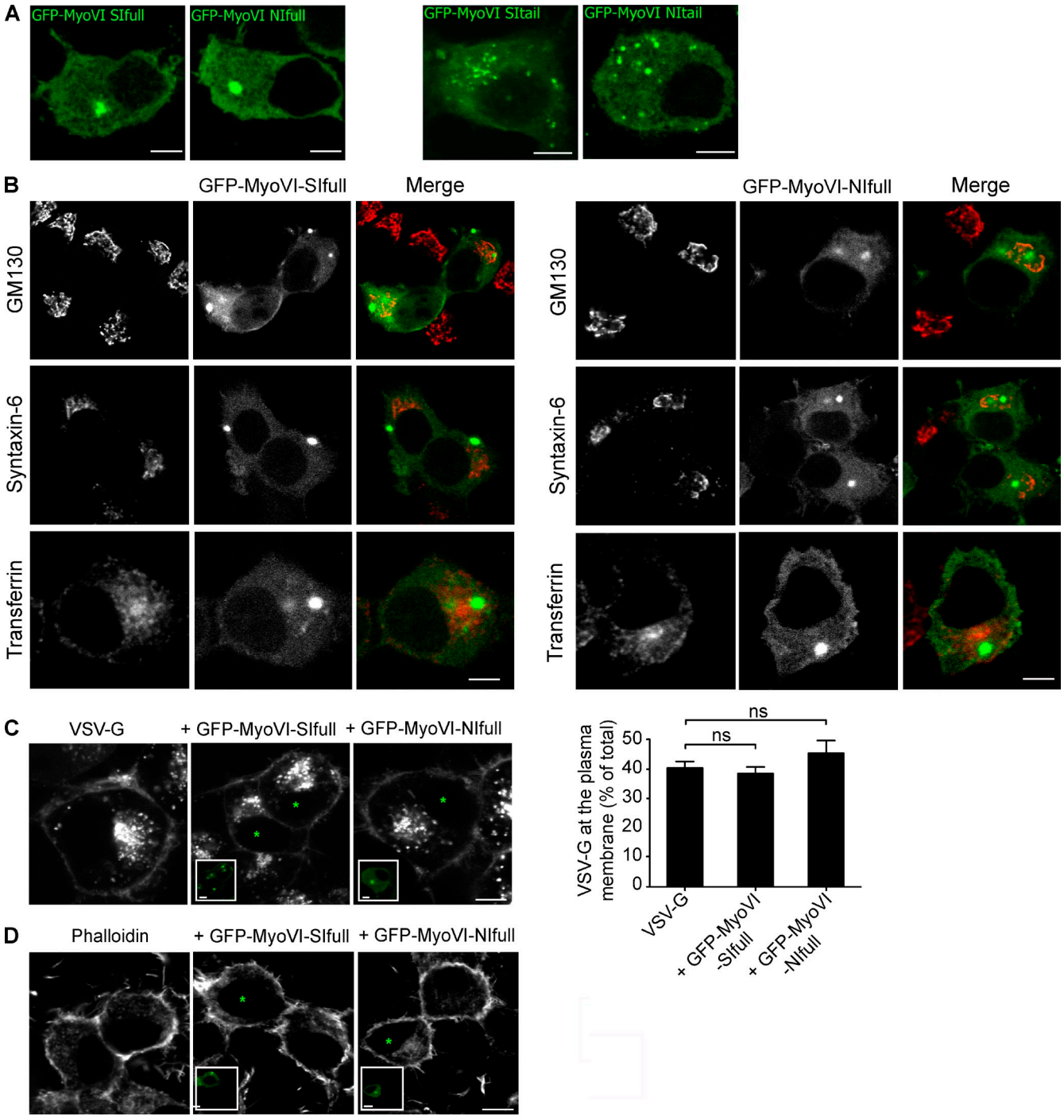

Figure S3. **GFP-MyoVI-full expression does not affect endocytic or exocytic pathways.** (A) Cells expressing the GFP-MyoVI proteins were fixed and imaged by confocal microscopy after a 48 h transfection. (B) Cells expressing GFP-MyoVI-SIfull (left) or GFP-MyoVI-NIfull (right) were imaged by confocal microscopy after immunolabeling with anti-GM130 (top) or anti–syntaxin-6 (middle) antibodies or after transferrin uptake (bottom). (C) Cells expressing VSV-G alone or coexpressing it with GFP-MyoVI-SIfull or GFP-MyoVI-NIfull were imaged by live-cell confocal microscopy. The amount of VSV-G at the plasma membrane was quantified and expressed as a percentage of total VSV-G. Error bars are means ± SEM. (D) Fixed control cells or cells expressing GFP-MyoVI-SIfull or GFP-MyoVI-NI were labeled with fluorescent phalloidin and imaged by confocal microscopy. (C and D) Green asterisks highlight transfected cells. Insets show the GFP channel. Bars, 5 µm.

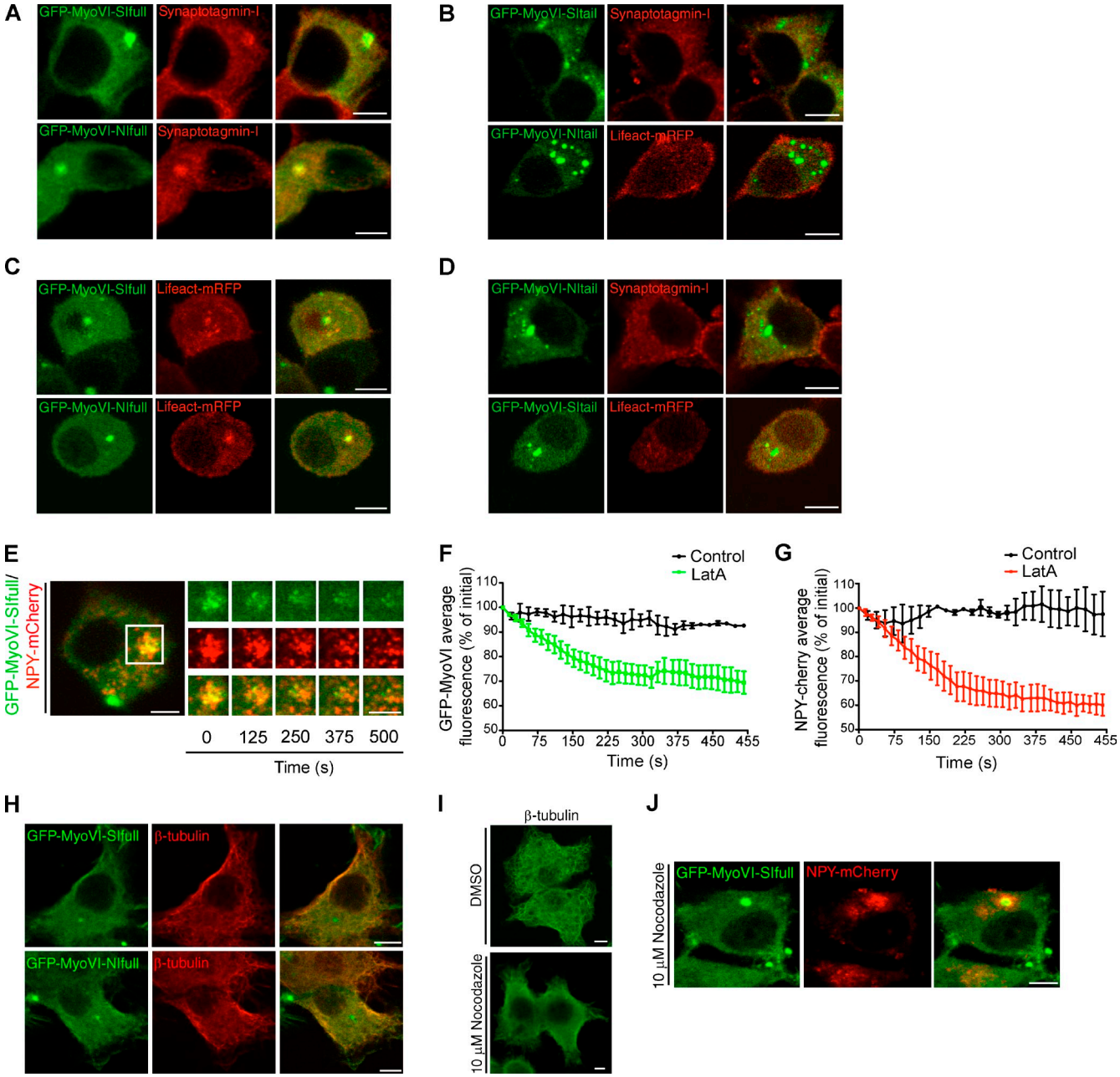

Figure S4. **GFP-MyoVI expression in PC12 cells reorganizes SGs in an F-actin–dependent, but not microtubule–dependent, manner.** (A and B) Cells expressing GFP-MyoVI-SIfull or GFP-MyoVI-NIfull (A) and GFP-MyoVI-SItail or GFP-MyoVI-NItail (B) were fixed and immunostained with the anti–Synaptotagmin-I antibody and imaged by confocal microscopy. (C and D) Cells coexpressing lifeact-mRFP with GFP-MyoVI-SIfull or GFP-MyoVI-NIfull (C) and lifeact-mRFP with GFP-MyoVI-SItail or GFP-MyoVI-NItail (D) were analyzed by live-cell confocal microscopy. (E) Cells coexpressing GFP-MyoVI-SIfull and NPY-mCherry were imaged using live-cell confocal microscopy after the addition of 6 µM latrunculin A. Single plane images were taken every 5 s, and pinholes were adjusted to obtain a 2-µm optical slice. Insets highlight the clustering of NPY-mCherry–positive SGs around the GFP-MyoVI–positive structures. (F and G) Quantification of the average fluorescence of GFP-MyoVI-SIfull structures (F) or NPY-mCherry clusters (G) in control cells (control) or latrunculin A–treated cells (LatA). Data represent means ± SEM (n = 3 experiments) and are expressed as a percentage of initial. (H) Cells expressing GFP-MyoVI-SIfull or GFP-MyoVI-NIfull were fixed and immunostained with anti–β-tubulin antibody and imaged by confocal microscopy. (I) PC12 cells were treated for 20 min with 10 µM nocodazole or vehicle (DMSO) at 37°C. After treatment, microtubule integrity was evaluated by immunostaining with anti–β-tubulin antibody (green) and imaging by confocal microscopy. (H) Cells coexpressing GFP-MyoVI-SIfull and NPY-mCherry were treated with 10 µM nocodazole for 20 min at 37°C, fixed, and imaged by confocal microscopy. Bars, 5 µm.

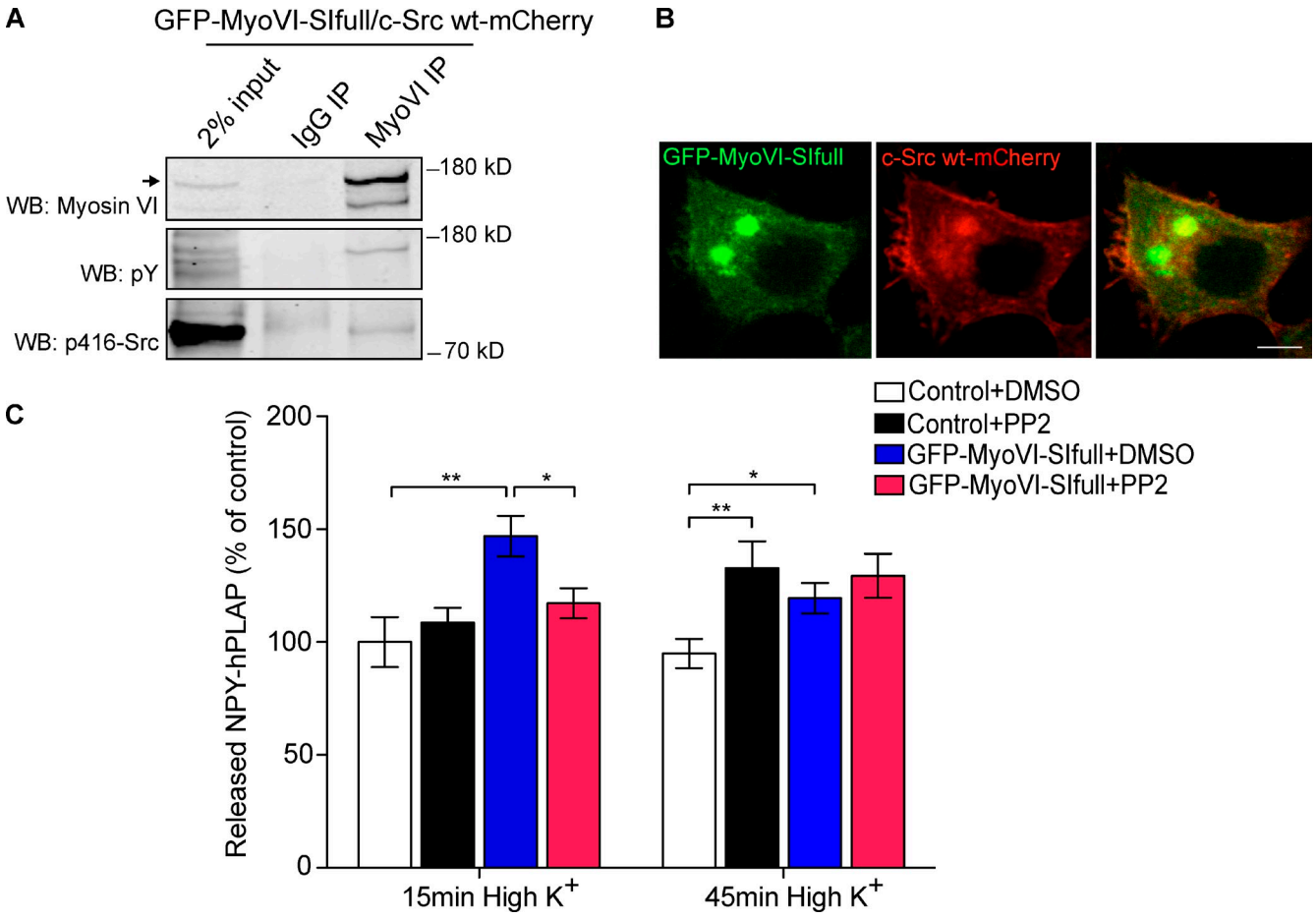

Figure S5. **The potentiation in SG-evoked release mediated by myosin VI SI is regulated by c-Src activity.** (A) Myosin VI immunoprecipitation (IP) from cells coexpressing GFP-MyoVI-SIfull with c-Src wild type (wt)–mCherry. (top) Western blotting (WB) against myosin VI. The arrow indicates the GFP-MyoVI-SIfull band. (middle) Phosphorylation of immunoprecipitated GFP-MyoVI-SIfull was evaluated by Western blotting using a general antiphosphotyrosine (pY) antibody. (bottom) c-Src wild type–mCherry expression was evaluated by Western blotting using a specific antiphosphorylated Src antibody (pY416-Src). (B) 72 h after transfection, PC12 cells coexpressing GFP-MyoVI-SIfull and c-Src wild type–mCherry were fixed and imaged by confocal microscopy. Bar, 5 µm. (C) PC12 cells coexpressing NPY-hPLAP with GFP (control) or GFP-MyoVI-SIfull were treated with 20 µM PP2 (PP2) or vehicle (DMSO) at 37°C for 15 min. After treatment, cells were incubated with PSS or PSS-high K^+ containing 20 µM PP2 or DMSO for 15 min (first round of stimulation). Supernatants were collected, and cells were washed and reincubated for 45 min (second round of stimulation) with the respective buffer. Released NPY-hPLAP is expressed as percentage of NPY-hPLAP released in control + DMSO cells. Values are expressed as means ± SEM of three independent experiments. *, $P < 0.05$; **, $P < 0.01$.

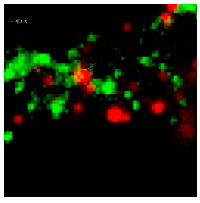

Video 1. **Myosin VI SI restricts the movement of SGs near the plasma membrane.** Myosin VI stable knockdown PC12 cells cotransfected with GFP-MyoVI-SIfull and NPY-mCherry were visualized after nicotine stimulation using time-lapse live-cell imaging using a TIRF microscope (Marianas and Everest; Intelligent Imaging Innovations, Inc.). The trajectory of a single NPY-mCherry–positive SG becomes restricted as its colocalization with GFP-MyoVI-SIfull increases. The video was compiled at two frames per second.

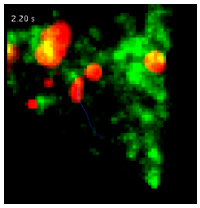

Video 2. **Myosin VI NI isoform lacks the ability to cage SG movement at the plasma membrane.** Myosin VI stable knockdown PC12 cells cotransfected with GFP-MyoVI-SIfull and NPY-mCherry were visualized after nicotine stimulation using time-lapse live-cell imaging using a TIRF microscope (Marianas and Everest; Intelligent Imaging Innovations, Inc.). The trajectory of a NPY-mCherry–positive SG is not restricted upon colocalization with GFP-MyoVI-NIfull. The video was compiled at two frames per second.

Table S1. **Selection of proteins identified by MALDI-TOF/TOF-MS**

Protein sequence accession number	Protein name	Species	Protein score	
			$-Ca^{2+}$	$+Ca^{2+}$
Q3MHM5	Tubulin β-2C chain	*Bos taurus* (bovine)	827	858
Q3ZBU7	Tubulin β-4 chain	*B. taurus* (bovine)	748	754
Q2T9S0	Tubulin β-3 chain	*B. taurus* (bovine)	430	502
Q2HJ81	Tubulin β-6 chain	*B. taurus* (bovine)	398	412
P81287	Annexin A5	*B. taurus* (bovine)	230	881
P63026	Vesicle-associated membrane protein 2	*B. taurus* (bovine)	63	81
Q13748	Tubulin α-2 chain	*Homo sapiens* (human)	-	800
P04272	Annexin A2	*B. taurus* (bovine)	-	299
Q9BUF5	Tubulin β-6 chain	*H. Sapiens* (human)	-	290
Q99867	Tubulin β-4q chain	*H. Sapiens* (human)	-	163
P46193	Annexin A1	*B. taurus* (bovine)	-	141
P20072	Annexin A7	*B. taurus* (bovine)	-	107
Q2KJD0	Tubulin β-5 chain	*B. taurus* (bovine)	904	1150
Q9NY65	Tubulin α-8 chain	*H. Sapiens* (human)	775	745
Q3MHM5	Tubulin β-2C chain	*B. taurus* (bovine)	734	965
Q6B856	Tubulin β-2B chain	*B. taurus* (bovine)	712	896
Q3ZBU7	Tubulin β-4 chain	*B. taurus* (bovine)	647	866
Q3T149	Heat shock protein β-1	*B. taurus* (bovine)	522	577
Q27975	Heat shock 70-kD protein 1A	*B. taurus* (bovine)	343	220
Q9BUF5	Tubulin β-6 chain	*H. Sapiens* (human)	256	370
P34933	Heat shock–related 70-kD protein 2	*B. taurus* (bovine)	235	171
P55063	Heat shock 70-kD protein 1L	*Rattus norvegicus* (rat)	-	185
Q99867	Tubulin β-4q chain	*H. Sapiens* (human)	189	191
P48616	Vimentin	*B. taurus* (bovine)	110	84
Q2HJ81	Tubulin β-6 chain	*B. taurus* (bovine)	-	478
Q61696	Heat shock 70-kD protein 1A	*Mus musculus* (mouse)	-	322
P13533	Myosin VI	*H. Sapiens* (human)	-	121

Peptide mass and fragmentation data were used to search against mammalian proteins in the SwissProt database using Mascot. Mascot protein scores >65 represent a >95% probability of a nonrandom match of peptide data. For Myosin VI, the human orthologous protein was found likely because of the absence of a bovine sequence entry for this protein in the database. Shown proteins were selected based on a previously identified role in vesicular trafficking or cytoskeletal function. Hyphens indicate no protein score.